Analyst

Accepted Manuscript

This article can be cited before page numbers have been issued, to do this please use: A. Roda, M. Guardigli, D. Calabria, M. M. Calabretta, L. Cevenini and E. Michelini, *Analyst*, 2014, DOI: 10.1039/C4AN01612B.

ROYAL SOCIETY OF CHEMISTRY

www.rsc.org/analyst

View Article Online
DOI: 10.1039/C4AN01612B

3D-printed device for smartphone-based chemiluminescence biosensor for lactate in oral fluid and sweat

Aldo Roda*[a,b], Massimo Guardigli[a], Donato Calabria[a,b], Maria Maddalena Calabretta[b], Luca Cevenini[a], Elisa Michelini [a,b]

[a]Department of Chemistry "G. Ciamician", University of Bologna, Via Selmi 2, Bologna, 40126, Italy

[b]INBB, Istituto Nazionale di Biostrutture e Biosistemi, Viale delle Medaglie d'Oro, 305, Roma, Italy

*Corresponding author
Prof. Aldo Roda
Laboratory of Analytical and Bioanalytical Chemistry
Department of Chemistry "G. Ciamician"
Alma Mater Studiorum - University of Bologna
Via Selmi 2
40126 Bologna Italy
tel: +39 051 343398 fax: +39 051 343398
E-mail: aldo.roda@unibo.it

View Article Online
DOI: 10.1039/C4AN01612B

Abstract

Increasingly, smartphones are used as portable personal computers, revolutionizing communication styles and entire lifestyles. Using 3D-printing technology we have made a disposable minicartridge thatcan be easily prototyped to turn any kind of smartphone or tablet into a portable luminometer to detect chemiluminescence derived from enzyme-coupled reactions. As proof-of-principle, lactate oxidase was coupled with horseradish peroxidase for lactate determination in oral fluid and sweat. Lactate can be quantified in less than five minutes with detection limits of 0.5 mmol/L (corresponding to 4.5 mg/dL) and 0.1 mmol/L (corresponding to 0.9 mg/dL) in oral fluid and sweat, respectively. The smartphone-based device shows adequate analytical performance to offer a cost-effective alternative for non-invasive lactate measurement. It could be used to evaluate lactate variation in relation to anaerobic threshold in endurance sport and for monitoring lactic acidosis in critical-care patients.

View Article Online
DOI: 10.1039/C4AN01612B

Introduction

Powerful yet affordable smartphones and tablets are playing an increasingly pivotal role in recreational activities and healthcare delivery. Hundreds of new applications (apps) are available to respond to the growing needs of end-users. In September 2013, the Food and Drug Administration (FDA) recommended that apps providing medical and scientific information be distinguished from those with diagnostic potential[1]. This distinction allows healthcare professionals and policy-makers to identify those apps which fall under the remit of the FDA. In contrast to conventional point-of-care (POC) devices, smartphone-based diagnostics eliminate the need for dedicated equipment. The smartphone itself can act as transducer or detector and perform data analysis, providing a final readout as simple as that of commercial glucometers.

Smartphones offer photography (still and video), location and other sensors (global positioning system [GPS], accelerometers, etc.), the long-distance transfer of information (data and images) via text messaging (Short Message Service - SMS), built-in apps (e-mail, calendar, document readers, etc.) and the possibility of developing or installing new apps, and wireless data service. Smartphones are thus ideal candidates for the development of simple and high-tech POC devices.

Till now, most health self-management apps have been limited to medication reminders, post-intervention questionnaires, therapy adjustments, and supportive messages for patients with chronic diseases like diabetes and asthma[2,3]. From a technical point of view, it is much more challenging to use smartphones as instruments for point-of-need analysis, e.g. immuno- or enzyme-based tests. Recent publications have successfully demonstrated the feasibility of this approach for monitoring biomarkers in biological fluids such as blood, saliva, and sweat using enzymatic reactions, paper-based immunoassays, and Lateral Flow Immunoassays (LFIAs)[4-6]. Mobile phone embedded cameras have already been exploited for fluorescence or colorimetric detection to measure analytes and detect infectious pathogens in environmental and clinical samples[7,9]. For example, Oncescu et al. have developed a smartphone accessory and a software app for measuring cholesterol levels in

View Article Online
DOI: 10.1039/C4AN01612B

blood, relying on the colorimetric changes induced by enzymatic reactions on a dry reagent paper strip[10]. Polymerase chain reaction (PCR) has also been integrated into a smartphone-assisted device by combining solar heating with microfluidics[11]. Bio-chemiluminescence (BL/CL) detection has not yet been systematically investigated for smartphone-based POC devices. In contrast to fluorescence detection, CL produces photons as a byproduct of a chemical reaction, with no need for a light source. This circumvents problems connected with background fluorescence and light scattering[12].

The main factor hampering the development of CL smartphone-embedded devices is that, despite the possibility of achieving low detection limits, CL is characterized by very low light emission intensities, especially when compared to fluorescence[13,14]. Therefore, CL detection requires highly sensitive detectors and must be performed in a darkbox to avoid interference from ambient light. The latter inconvenience can be easily circumvented by adopting a light-proof minicase. However, we have previously reported that adequate sensitivity for performing BL/CL measurements is possessed by relatively inexpensive thermoelectrically-cooled Charge-Coupled Device (CCD) cameras designed for astronomical applications and by complementary metal-oxide semiconductor (CMOS) sensors integrated into smartphones[15,16].

The monitoring of lactate levels is relevant for diabetes control, sport medicine, and for critical-care patients at risk of heart attack. There is a close relationship between lactate accumulation and muscle fatigue. Reaching of anabolic threshold can be easily assessed by lactate monitoring. Lactate can be measured in different biological fluids, including blood, saliva, and sweat[17]. Several lactate biosensors based on different detection principles (chemiluminescence and amperometric detection) have already been developed to monitor the endurance performance of athletes via lactate detection in sweat and blood[18,21].

Here, we report the development of a smartphone-based device for non-invasive and easy monitoring of the endurance performance of athletes via lactate detection. This biosensor relies on CL detection and exploits the lactate-oxidase (LOx) catalyzed reaction coupled with the enhanced

View Article Online
DOI: 10.1039/C4AN01612B

luminol/H_2O_2/horseradish peroxidase (HRP) CL system. The device was made with low-cost 3D printing technology and includes a disposable analytical minicartridge, a mini dark box to avoid interference from ambient light during measurement, and a holder to connect the dark box to a smartphone. We have demonstrated that the device could be used for the reliable real-time measurement of lactate levels in oral fluid and sweat samples. In principle, this biosensor could also find application in detecting other analytes of clinical interest in oral fluid and sweat.

Materials and methods

Chemicals

Peroxidase (type VI-A from horseradish, 1080 U/mg protein), L-lactate oxidase (from *Pediococcus sp.*, 50 U/mg protein), L-lactate sodium salt, L-histidine monohydrochloride monohydrate, mucin (type II from porcine stomach) and urea were supplied from Sigma Aldrich (St. Louis, MO). Sodium chloride, disodium hydrogen orthophosphate anhydrous, sodium dihydrogen orthophosphate monohydrate were supplied from Carlo Erba Reagents S.r.l. (Milano, Italy). The luminol-based HRP substrate Super Signal® West Dura was from Thermo Scientific (Waltham, MA). Artificial sweat was prepared according to the International Standard Organization (ISO105-E04-2008E) and the British Standard (BS EN1811-1999) with a pH 5.5 [0.05 % (w/v) L-histidine monohydrochloride monohydrate, 0.50 % (w/v) NaCl, 0.22 % (w/v) $NaH_2PO_4 \cdot 2H_2O$)][22]. Artificial saliva at pH 7.2 was prepared by dissolving 0.6 mg/mL Na_2HPO_4, 0.6 mg/mL anhydrous $CaCl_2$, 0.4 mg/mL KCl, 0.4 mg/mL NaCl, 4.0 mg/mL mucin and 4.0 mg/mL urea in deionised water according to Tlili et al.[23]. The fluorometric lactate enzymatic assay in the standard 96-well microtiter plate format (EnzyFluo™ L-Lactate Assay Kit) was bought from BioAssay Systems, Hayward, CA and used according to the manufacturer's instructions.

Smartphone camera performance comparison

View Article Online
DOI: 10.1039/C4AN01612B

The performance of the smartphone (Samsung Galaxy SII Plus, Samsung Group, Seoul, South Corea) embedded camera was compared with that of a benchtop low-light luminograph equipped with a thermoelectrically-cooled CCD camera (LB 981 Night Owl, Berthold Technologies GmbH & Co. KG, Bad Wildbad, Germany). A battery-powered blue LED (λ_{max} = 466 nm) was used as a model source. To evaluate the response of the cameras to different light intensities, the emission of the LED was attenuated using Kodak Wratten 2 neutral density (ND) filters of known optical density (Edmund Optics, Barrington, NJ). Image exposure time was set to 30 s for both cameras. For evaluation of the signal-to-noise (S/N) ratios of the images, signals (S) were calculated by averaging the pixel intensity over the LED image area, while noise (N) was taken as the standard deviation of the mean pixel intensity in a dark image area.

3D printed analytical device fabrication

The analytical device (Fig. 1) is made of black and transparent acrylonitrile-butadiene-styrene (ABS) polymer and was produced using a low-cost commercial 3D printer (Replicator 2X Desktop 3D Printer, MakerBot Industries, New York, NY). The device was designed using the open-source Tinkercad browser-based 3D design platform (Autodesk, Inc). Files were exported as .stl files and MakerWare v.2.4 software, an algorithm that slices digital into thin layers for 3D printing, was used to define printing options and settings. The device consists of three separate components: (a) a disposable analytical cartridge, (b) a mini dark box, and (c) a smartphone adapter.

The analytical cartridge (42 mm x 28 mm) contains two reaction chambers (sample and control reaction chamber) (diameter 4 mm, depth 5 mm) with small 4-mm-diameter disks of nitrocellulose membrane, onto which LOx and HRP are co-absorbed. The enzyme amounts immobilized on the disks were as follows: LOx 1.0 U (for sweat analysis) or 0.02 U (for saliva analysis), horseradish peroxidase 0.1 U. Two reagents' reservoirs adjacent to each reaction chamber (diameter 4 mm, depth 3 mm) contain the luminol/enhancer solution of the Super Signal® West Dura HRP CL reagent (10 μL) and a 0.1 M, pH 7.0 buffer phosphate solution (10 μL). The buffer reservoir

View Article Online
DOI: 10.1039/C4AN01612B

adjacent to the control reaction chamber also contains L-lactate in artificial saliva or sweat matrices (the same volume of the sample analyzed: 15 µL) to provide an adequate control (2.0 mmol/L and 4.0 mmol/L lactate for saliva and sweat, respectively). The sample reaction chamber is connected to a sample insertion well (diameter 9 mm, depth 4 mm), by which the biological fluid to be analyzed can be added. The cartridge is covered by a cartridge lid that avoids fluid leakage during storage and use of the cartridge. The lid can be fitted on the cartridge in two different orientations. When the cartridge is not in use, two lid pins are inserted in the reaction chambers, blocking the channels connecting the reaction chambers to the reagents' reservoirs and avoiding premature mixing of the reagents. During the analysis, the lid is fitted on the cartridge in the opposite orientation: the reagents can freely flow from the reservoirs to the reaction chambers and two transparent ABS pins are inserted in the reaction chambers, allowing measurement of the CL emission. The lid holds a further pin with a patch (9 mm diameter, 2 mm thickness) right by the sample insertion well, which allows a fixed volume of sample to be transferred to the sample reaction chamber.

The mini dark box contains the analytical cartridge during the measurement, assuring its correct positioning and avoiding interference from ambient light.

The smartphone adapter holds the mini dark box and can be snapped onto the smartphone to correctly position the dark box in relation to the smartphone embedded camera. The adapter includes a plano-convex plastic lens (diameter 6 mm, focus 12 mm), which focuses the image of the reaction chambers of the cartridge onto the smartphone camera.

Assay procedure

Oral fluid and sweat are collected by unsnapping the lid from the cartridge and applying the patch on the lid to the skin of the forearm or forehead or to the tongue, respectively. The lid is then inserted into the cartridge in the measurement orientation by applying a slight pressure. This closes the cartridge and drives a fixed volume of sample (15 µL) into the reaction chamber. The CL enzymatic reaction is then triggered after sample injection with two simple flicks, which drive the

View Article Online
DOI: 10.1039/C4AN01612B

buffer phosphate solution (and the L-lactate standard for the control) and the CL reagent from the reservoirs to the reaction chambers. The cartridge is then inserted into the mini dark box camera, which is already snapped to the smartphone. The light signal is measured by the smartphone camera. Suitable smartphone photography apps are used to control exposure time (which must be long enough to achieve the required detectability) and for image handling. For Android-based smartphones, we used the Camera FV-5 (Android) Lite app to perform long (60 s) image acquisitions. Quantitative analysis of the CL images was performed using the open source software ImageJ v.1.46 (National Institutes of Health, Bethesda, MD). Regions of interest (ROIs) corresponding to the sample and control detection chambers, as well as a ROI of the same dimension in a dark area of each image for subtraction of the background signal, were selected. Light emissions were quantified as raw integrated densities. GraphPad Prism v. 5.04 (GraphPad Software, Inc., La Jolla, CA) was used to plot CL signal as a function of lactate concentration and for least-squares fitting of calibration curves.

Results and discussion

The aim of this work was to develop a portable lactate CL biosensor for assessing L-lactate levels in oral fluid and sweat, based on the coupling of the enzymatic oxidation of lactate catalyzed by L-lactate oxidase with the luminol/H_2O_2/HRP CL system. We designed a simple device using disposable analytical cartridges to allow measurement of the light produced by the enzyme reaction using a smartphone embedded camera. This device exploits the backside-illumination complementary metal-oxide semiconductor (BI-CMOS) sensors integrated into modern smartphones. These offer improved low-light performance in comparison to conventional front-illuminated CMOS sensors. The device also takes advantage of low-cost 3D printing technologies, which allowed the rapid prototyping and production of device components.

Smartphone camera performance

View Article Online
DOI: 10.1039/C4AN01612B

Chemiluminescent reactions produce weak light emissions. An estimation of the light detectability required to satisfy the analytical requirement of the device can be done as follows. According to the L-lactate content of oral fluid with a physiological range of 0.1-2.5 mmol/L[24] and sweat with values that vary up to 25 mmol/L according to an individual's metabolism and physical performance[25,26], we need a minimum L-lactate detectability of the order of 0.1 mmol/L. At this concentration level, a 15-μL sample of biological fluid contains as low as 1 nmole of L-lactate, which will be converted by L-lactate oxidase to the same amount of hydrogen peroxide. Assuming a quantum efficiency of the luminol/H_2O_2/HRP CL system of the order of 0.01, the HRP-catalyzed reaction of the hydrogen peroxide with luminol will produce about 10^{13} photons, which should be imaged and detected by the smartphone embedded camera. By taking into account the system optics and geometry, it could be estimated that the light collection efficiency of the device (the fraction of the photons emitted by the sample that effectively reach the CMOS sensor) should be of the order of 5%. Finally, by considering that the image of a reaction chamber of the cartridge covers an area of about 2.8 x 10^5 image pixels, we concluded that the minimum light detectability required is around 10^3 photons/image pixel. We preliminarily compared the performance of the smartphone embedded camera to that of a low-light luminograph equipped with a thermoelectrically-cooled CCD camera using a model LED light source. Both systems showed a good correlation between measured signals and light intensities. However, for any given intensity of the model light source, the S/N ratios of the luminograph images were about three orders of magnitude higher than those of the images acquired with the smartphone embedded camera (data not shown). Since the S/N ratio determines light detectability, it could be concluded that the minimum light intensity detectable with the smartphone embedded camera is about three orders of magnitude higher than that of the low-light luminograph. The lower light detectability of the smartphone embedded camera could be ascribed to several factors, such as the smaller pixels (1.4 × 1.4 μm^2 *vs* 9 × 9 μm^2) and the absence of a sensor cooling system, which resulted in a higher thermal noise.

Nevertheless, the sensitivity of the smartphone camera is still adequate for the quantitative

View Article Online
DOI: 10.1039/C4AN01612B

measurement of analytes through enzyme-catalyzed CL reactions, at least for species present at relatively high concentrations, providing a careful optimization of the analytical system.

Analytical device design

The analytical device obtained by low-cost 3D printing technology[27] is designed to be snapped onto a Samsung Galaxy SII smartphone, allowing a simple one-step analytical procedure after introducing a sample into the cartridge. The 3D printing technology allows rapid prototyping of the analytical device (particularly the adapters, which are designed to fit a specific smartphone model according to its size and the camera position). In principle, the system could also be adapted to tablets. Due to their larger screens, tablets may be preferable to smartphones for applications requiring image visualization (e.g. cell imaging or lateral flow immunochromatographic analyses).

The analytical cartridge is the critical component. It allows a simple one-step analytical procedure in which a defined amount of sample is introduced into the cartridge and mixed with the enzymes and other reactants. Since enzyme reactions (thus CL emission intensities) are affected by temperature and other environmental variables, the cartridge includes a suitable control to improve assay accuracy and reproducibility.

To fulfill these requirements, all the reagents required for the analysis are already contained in the analytical cartridge, either in the reagents' reservoirs or, in the case of the enzymes LOx and HRP, immobilized in the dry state on a nitrocellulose membrane. The analytical cartridge contains two separate reaction chambers (each of them connected to its own reagents' reservoirs), in which the sample and a lactate control are analyzed in parallel. For quantitative analysis, the CL signal of the sample is normalized to that of the control (2.0 mmol/L or 4.0 mmol/L lactate for oral fluid or sweat, respectively). In addition, the control sample is prepared in artificial oral fluid or artificial sweat to take into account the effect of the sample matrix on the intensity of the CL signal. The whole analytical procedure is simply controlled by acting on the cartridge lid. Removal of the lid allows the reagents to flow from the reservoirs to the reaction chambers. The lid is also used for

View Article Online
DOI: 10.1039/C4AN01612B

collecting and transferring oral fluid or sweat samples: upon collection of the sample in the lid patch, inserting the lid into the cartridge drives a fixed volume of sample (15 μL) into the sample reaction chamber. Afterwards, shaking the cartridge transfers the reagents into the reaction chambers and initiates the enzyme reactions leading to light emission.

Assay optimization

Due to the relatively low sensitivity of the embedded smartphone cameras, experimental conditions (enzymes concentrations, pH, sample volumes, etc.) were optimized to provide a strong CL signal and a relatively fast emission kinetics.

Enzyme immobilization. The enzymes required for the assay enzymes were co-absorbed on small nitrocellulose membrane disks (diameter 4 mm) placed in the reaction chambers of the analytical cartridge. Nitrocellulose membranes are commonly used for protein absorption because of their high binding capacity and low background staining, and because physical immobilization of enzymes on membranes is easy and does not affect enzyme activity as much as covalent bonding or cross-linking methods. The enzyme amounts were optimized to obtain intense CL signals and fast reaction kinetics (rapid conversion of lactate to pyruvate and H_2O_2 followed by the HRP-catalyzed oxidation of luminol by H_2O_2) even in the presence of large amounts of lactate. Because of the higher lactate concentrations in sweat, different optimal amounts of LOx were individuated for the two matrices: cartridges for sweat analysis were loaded with a larger amount of LOx (1.0 U) than those for analysis of oral fluid (0.02 U). But both cartridges contained the same amount of HRP (0.1 U).

Emission kinetics. To achieve a low detection limit, it was necessary to collect a large fraction of the light emitted by the CL enzyme reaction. In addition to optimizing the geometry of the device, a suitable integration time was selected for acquiring the CL signal from the cartridge. The analysis of the kinetic profiles of the CL emission in the presence of different amounts of lactate showed the light emission kinetics emission slightly depended on the concentration of lactate. The maximum

View Article Online
DOI: 10.1039/C4AN01612B

emission intensities were obtained at times varying from 15 s (for the lowest lactate concentrations) to 30 s (for the highest ones) upon introduction of the sample and triggering of the enzymatic reactions (Fig. 2). According to the kinetics of the reaction, an integration time of 60 s upon insertion of the cartridge into the device was chosen to collect at least 90% of the overall light emission independently from the lactate concentration of the sample.

Matrix effect. To perform a reliable measurement of lactate in real samples, the possible interference of oral fluid and sweat matrices on the CL signal were evaluated. To study the matrix effect, we compared the CL emissions obtained for samples with low (1 mmol/L) and high (8 mmol/L) lactate levels prepared in artificial oral fluid (or sweat) and in phosphate buffer. The sample matrices caused a significant decrease of the intensity of the CL signal (about 60-70% and 40% for oral fluid and sweat, respectively). A similar reduction of the CL signal was also observed by analyzing real samples prepared by spiking oral fluid and sweat samples with negligible (less than 0.1 mmol/L) lactate concentrations with known amounts of lactate. To take into account the matrix effect, the calibration curves used for the quantitative analysis of lactate, as well as the control samples in the cartridges, were obtained using lactate solutions prepared in artificial oral fluid and sweat. This allowed a reliable evaluation of lactate concentrations in real samples as reported below.

Analytical performance

Fig. 3B and 3C show the calibration curves obtained by analyzing standard lactate solutions prepared in artificial oral fluid and sweat following the optimized analytical procedure described above. Eeach measure was performed in a separate cartridge and the CL signal obtained for the sample was normalized to the value recorded for the control (2.0 and 4.0 mmol/L for oral fluid and sweat, respectively) in the same cartridge. Signal normalization is expected to increase assay reproducibility by reducing the effect of environmental variables (e.g. temperature) and other factors on the intensity of the CL signal. The CL signal showed a nonlinear dependence on lactate

View Article Online
DOI: 10.1039/C4AN01612B

concentration. To perform quantitative analysis, calibration curves were obtained by fitting the experimental data with the empirical equation $y = a(1-e^{-bx})$, where y and x represent the CL signal and the lactate concentration, respectively.

According to the calibration curves, limits of detection (LOD) of 0.5 mmol/L (corresponding to 4.5 mg/dL) and 0.1 mmol/L (corresponding to 0.9 mg/dL) of lactate were obtained in oral fluid and sweat, respectively. In addition, the smartphone-based lactate biosensor allowed measurement of lactate in oral fluid and sweat along the entire range of physiological values.

Assay validation

To validate the assay, oral fluid and sweat samples were analyzed in parallel with the smartphone-based lactate biosensor and with a commercial L-lactate enzymatic assay based on the lactate dehydrogenase-catalyzed oxidation of lactate, in which the formed NADH reduces a probe into a highly fluorescent product. Fluorescence detection allowed us to achieve a LOD (1 μmol/L) lower than that of colorimetric lactate enzymatic assays. Samples could thus be analyzed upon dilution to avoid any matrix effect. Fig. 4 compares the concentrations measured in oral fluid and sweat samples, which indicated a good correlation between the effective concentration of lactate in the samples and the results obtained with the smartphone-based lactate biosensor.

Application

Lactate is constantly produced by glucose metabolism, even under resting conditions. However, lactate levels increase during intense physical exercise, thus they are an indicator of performance development in training regimes, especially endurance sports. To demonstrate the applicability of the smartphone-based biosensor for monitoring lactate levels during physical exercise, we measured the lactate in sweat during running track performed by a volunteer. Fig. 5 reports the sweat lactate profile measured in the volunteer and obtained by collecting (as described in the Materials and Methods section) and immediately analyzing sweat sampled at regular intervals (10 minutes). The

View Article Online
DOI: 10.1039/C4AN01612B

data clearly showed the increase in lactate concentration during the exercise activity, demonstrating the possibility of real-time monitoring of lactate levels.

Measurement of lactate in sweat or oral fluid also allowed assessment of the athlete's anaerobic threshold, i.e. the exercise level above which pyruvate production due to anaerobic metabolism is faster than pyruvate consumption due to aerobic metabolism. Above this threshold, accumulation of unused pyruvate and its conversion into lactate causes acidosis, reducing exercise endurance. Instead of performing a lactate quantitative analysis to assess the reaching of the anaerobic threshold, the CL signal obtained for the sample could simply be compared to that of the internal control, providing that the lactate concentration in the control corresponded to the anaerobic threshold level in sweat or oral fluid. As an example of this approach, Fig. 6 shows the results obtained using cartridges containing a 4.0 mmol/L lactate control sample for the analysis of sweat samples with lactate concentrations of about 2.0 and 8.0 mmol/L, respectively. In accordance with the calibration curves, the CL signal intensities were not linearly proportional to the analyte concentration. But sweat samples with lactate concentrations below and above the control sample could easily be discriminated. This approach could therefore allow a simple assessment of the reaching of the anaerobic threshold by an athlete as a result of continual exercise at high intensity. However, the lactate level corresponding to the anaerobic threshold may present significant inter-individual variation, which will also depend on the fitness of the subject. This approach may therefore require the development of a series of cartridges, in which control samples cover a range of lactate concentrations.

Conclusions

We have developed a smartphone-based chemiluminescence biosensor that exploits mobile technology and 3D printing, two affordable technologies that are revolutionizing everyday life, to obtain a sort of "portable mini-laboratory". The core element of this mini-lab is a disposable plastic cartridge for enzymatic assays and a smartphone accessory that can be easily tailored to different

View Article Online
DOI: 10.1039/C4AN01612B

smartphones and tablets. As proof-of-concept, we developed an assay to monitor lactate levels in sweat and oral fluid. This device shows adequate analytical performance, offering a cost-effective alternative for non-invasive lactate measurement to monitor the intensity and maximum duration of athletes' performance during physical exercise.

The device could also be adapted to a variety of other assays that require simplicity, low-cost, portability, and flexibility. The data reported in this work clearly demonstrate that combining chemiluminescence as a detection principle with a smartphone camera as a detector is an ideal strategy for developing simple, sensitive, and portable analytical devices. In addition, ad hoc applications can easily be implemented to store the analyte values and handle data elaboration, providing the end user with a simple readout (e.g. analyte concentration in comparison to physiological ranges or a sort of "traffic light"). This smart test could activate a green light when the analyte is within physiological values (personalized to the individual according to results stored in the memory), amber light when concentrations are reaching the threshold, and red light (or a voice alert warning) for higher values. Moreover, the device could be used to monitor lactic acidosis to prevent heart attacks in critical-care patients.

View Article Online
DOI: 10.1039/C4AN01612B

References

1. Food and Drug Administration: Mobile medical applications: guidance for industry and Food and Drug Administration staff. Available at http://www.fda.gov/downloads/MedicalDevices/.../UCM263366.pdf
2. T. de Jongh, I. Gurol-Urganci, V. Vodopivec-Jamsek, J, Car and R. Atun, *Cochrane Database Syst. Rev.*, 2012, **12**, CD007459.
3. S. Silow-Carroll, and B. Smith, *Issue Brief. (Commonw Fund.)*, 2013, **30**, 1-10.
4. L. Sangdae, K. Giyoung, and M. Jihea, *Sensors (Basel)*, 2013, **13**, 5109-5116.
5. V. Oncescu, M. Mancuso, and D. Erickson, *Lab Chip*, 2014, **14**, 759-763.
6. D. Erickson, D. O'Dell, L. Jiang, V. Oncescu, A. Gumus, S. Lee, M. Mancuso, and S. Mehta, *Lab Chip*, 2014, **14**, 3159-3164.
7. G. H. Chen, W.Y. Chen, Y. C. Yen, C. W. Wang, H. T. Chang, and C.F. Chen. *Anal. Chem.*, 2014, **86**, 6843-6849.
8. E. Petryayeva, and W. R. Algar, *Anal. Chem.*, 2014, **86**, 3195-3202..
9. C.C. Stemple, S.V. Angus, T.S. Park, and J.Y. Yoon, *J. Lab. Autom.*, 2014, **19**, 35-41.
10. V. Oncescu, D. O'Dell, and D. Erickson, *Lab Chip*, 2013, **13**, 3232-3238.
11. L. Jiang, M. Mancuso, Z. Lu, G. Akar, E. Cesarman, and D. Erickson, *Sci. Rep.*, 2014, **20**, 4137-4141.
12. A. Roda, M. Guardigli, E. Michelini and M. Mirasoli, *Anal. Bioanal. Chem.*, 2009, **393**, 109-123.
13. C.A. Marquette, B.P. Corgier, and L. J. Blum, *Bioanalysis*, 2012, **4**, 927-936.
14. S. Pennathur, D.K. Fygenson, *Lab Chip*, 2008, 8, 649-652.
15. A. Roda, L. Cevenini, S. Borg, E. Michelini, M. M. Calabretta, and D. Schüler, *Lab Chip*, 2013, **13**, 4881-4889.

View Article Online
DOI: 10.1039/C4AN01612B

16. A. Roda, E. Michelini, L. Cevenini, D. Calabria, M.M. Calabretta, and P. Simoni, *Anal. Chem.*, 2014, **86**, 7299-7304. .

17. G. G. Guilbault, G. Palleschi, and G. Lubrano, *Biosens Bioelectron.*, 1995, **10**, 379-392.

18. P.J. Lamas-Ardisana, O.A. Loaiza, L. Añorga, E. Jubete, M. Borghei, V. Ruiz, E. Ochoteco, G. Cabañero, and H.J. Grande, *Biosens. Bioelectron.*, 2014, **56**, 345-351.

19. H. Nakamura, Y. Murakami, K. Yokoyama, E. Tamiya, I. Karube, M. Suda, and S. Uchiyama,, *Anal. Chem.*, 2001, **73**, 373-378.

20. A. Hemmi, K. Yagiuda, N. Funazaki, S. Ito, Y. Asano, T. Imato, K. Hayashi, and I. Karube, *Anal. Chim. Acta*, 1995, **316**, 323-327.

21. M. M. Rahman, M. J. Shiddiky, M. A. Rahman, and Y. B. Shim, *Anal. Biochem.*, 2009, **384**, 159-165.

22. K. Kornphimol, S. Sujittra, B. Kanittha, K. Wiyong, and M. Rawiwan, *Part. Fibre Toxicol.*, 2010;, **7**,1-9.

23. C. Tlili, L.N. Cella, V.N. Myung, V. Shetty and A. Mulchandani, *Analyst*, 2010, **135**, 2637–2642.

24. N. W. Tietz, Clinical Guide to Laboratory Tests, W.B. Saunders Company, Philadelphia, PA, 3rd edn, 1995.

25. J.M. Green, R.C. Pritchett, T.R. Crews, J.R. McLester Jr, and D.C. Tucker, *Eur. J. Appl. Physiol.*, 2004, **91**, 1-6.

26. W. Jia, A.J. Bandodkar, G. Valdés-Ramírez, J.R. Windmiller, Z. Yang, J. Ramírez, G. Chan, and J. Wang, *Anal. Chem.*, 2013, **85**, 6553-6560.

27. B. C. Gross, J.L. Erkal, S.Y. Lockwood, C. Chen, and D.M. Spence, *Anal Chem.*, 2014, **86**, 3240-3253.

View Article Online
DOI: 10.1039/C4AN01612B

Figure legends

Figure 1. The 3D printed analytical device made of black and transparent ABS polymer consisting of three separate components: a disposable analytical cartridge (42 mm x 28 mm) with two reaction chambers, two reagents' reservoirs and a sample chamber, a mini dark box, and a smartphone adapter. (A) Cross-sections of the analytical cartridge and the cartridge lid and (B) horizontal section of the analytical cartridge showing the internal chambers and fluidic connections. (C) Photo of the cartridge-lid assembly and of the mini dark box and smartphone adapter.

Fig. 2 Chemiluminescence kinetic profiles obtained for the analysis of artificial sweat samples containing different lactate concentrations in the range 0.1–20 mmol/L. Kinetics measurements were performed by imaging the analytical cartridge using an electron multiplying charge coupled device (EM-CCD) camera (ImagEM-X2, Hamamatsu, Japan).

Fig. 3 (A) Images obtained by analyzing lactate standard solutions in artificial oral fluid and calibration curves obtained in (B) oral fluid and (C) sweat. Chemiluminescence signals were normalized to the CL signals obtained for the control samples (2.0 and 4.0 mmol/L for oral fluid and sweat, respectively) of the same cartridge. The least-square fitting of the experimental data according to the empirical equation $y = a(1-e^{-bx})$ is also shown (R^2 = 0.98-0.99). Data points represent the mean ± SD of three replicates.

Fig. 4 Comparison of the lactate concentrations measured in (A) oral fluid and (B) sweat samples using the smartphone-based lactate biosensor and a fluorometric L-lactate enzymatic assay kitperformed in the standard 96-well microtiter plate format (EnzyFluo™ L-Lactate Assay Kit). Eeach data represents the mean ± SD of three replicates.

Fig. 5 (A) Lactate concentrations in sweat measured in real-time during the exercise activity performed by a volunteer (each data represents the mean ± SD of three replicates). Sweat sampled, collected by unsnapping the lid from the cartridge and applying the patch on the lid to the skin of the forearm or forehead, were taken at 10 min intervals and immediately analyzed. (B) Picture of a representative CL acquisition with the smartphone.

View Article Online
DOI: 10.1039/C4AN01612B

Fig. 6 (A) CL images of cartridges with a 4.0 mmol/L lactate control obtained for the analysis of sweat samples with lactate concentrations of 2.0 and 8.0 mmol/L. Sweat samples were assayed in the lower reaction chamber, while control samples were analyzed in the upper one. (B) Relative CL signals of the sweat samples (normalized to the CL signal of the control, mean ± SD of three replicates).

View Article Online
DOI: 10.1039/C4AN01612B

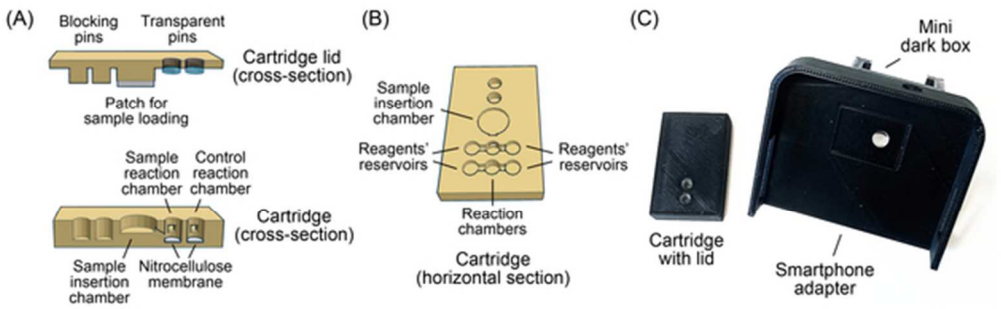

Figure 1. (A) Cross-sections of the analytical cartridge and the cartridge lid and (B) horizontal section of the analytical cartridge showing the internal chambers and fluidic connections. (C) Photo of the cartridge-lid assembly and of the mini dark box and smartphone adapter.
53x16mm (300 x 300 DPI)

View Article Online
DOI: 10.1039/C4AN01612B

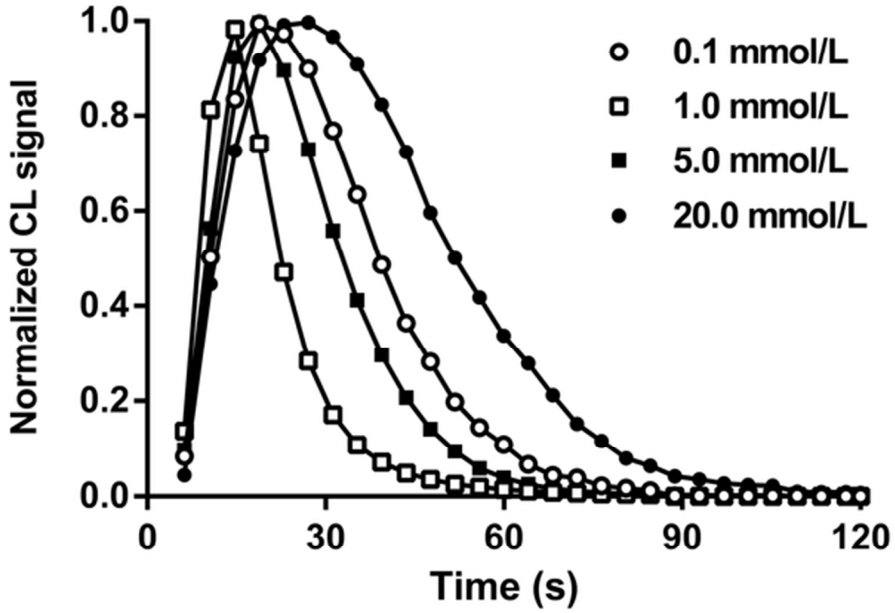

Fig. 2 Chemiluminescence kinetic profiles obtained for the analysis of artificial sweat samples containing different lactate concentrations in the range 0.1 – 20 mmol/L.
57x39mm (300 x 300 DPI)

View Article Online
DOI: 10.1039/C4AN01612B

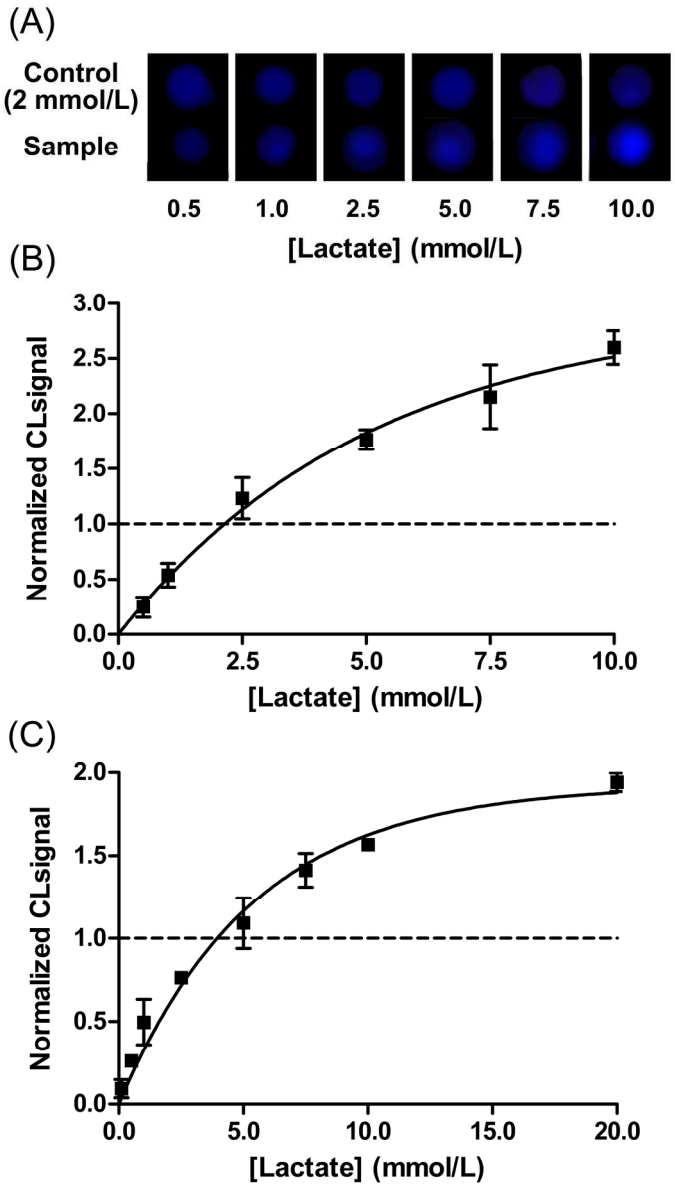

Fig. 3 (A) Images obtained by analyzing lactate standard solution in artificial oral fluid and calibration curves obtained in (B) oral fluid and (C) sweat. Chemiluminescence signals were normalized to the CL signals obtained for the control samples of the same cartridge. The least-square fitting of the experimental data according to the empirical equation y = a(1-e-bx) is also shown (R2 = 0.98-0.99). Data points represent the mean ± SD of three replicates.
144x250mm (300 x 300 DPI)

View Article Online
DOI: 10.1039/C4AN01612B

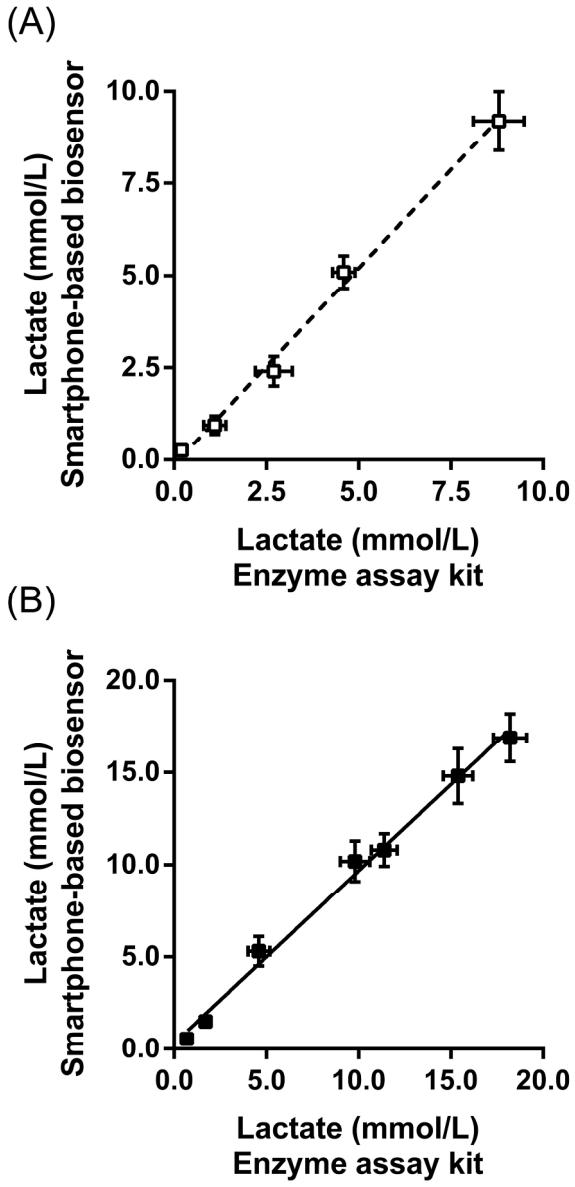

Fig. 4 Comparison of the lactate concentrations measured in (A) oral fluid and (B) sweat samples using the smartphone-based lactate biosensor and the fluorometric lactate enzymatic assay kit (each data represents the mean ± SD of three replicates.
156x296mm (300 x 300 DPI)

View Article Online
DOI: 10.1039/C4AN01612B

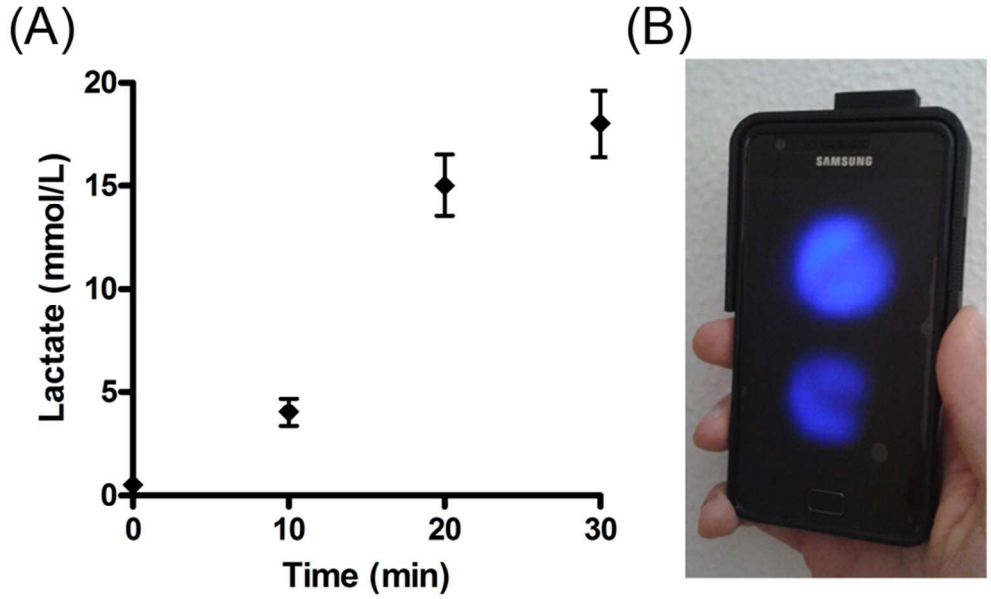

Fig. 5 (A) Lactate concentrations in sweat measured in real-time during the exercise activity performed by the volunteer (each data represents the mean ± SD of three replicates). (B) Picture of a representative CL acquisition with the smartphone.
82x50mm (300 x 300 DPI)

View Article Online
DOI: 10.1039/C4AN01612B

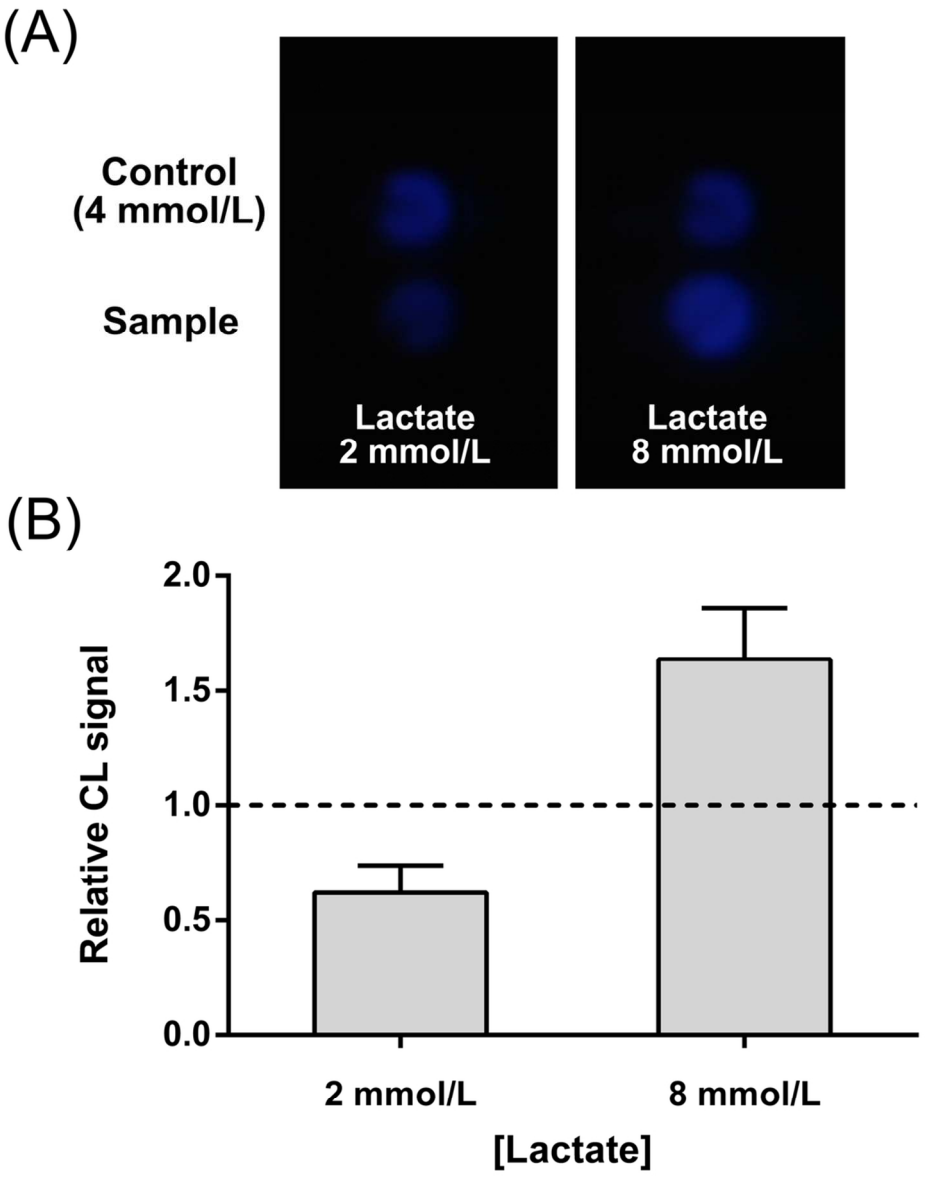

Fig. 6 (A) CL images of cartridges with a 4.0 mmol/L lactate control obtained for the analysis of sweat samples with lactate concentrations of 2.0 and 8.0 mmol/L. Sweat samples were assayed in the lower reaction chamber, while control samples were analyzed in the upper one. (B) Relative CL signals of the sweat samples (normalized to the CL signal of the control, mean ± SD of three replicates).
101x124mm (300 x 300 DPI)